J. Fluid Mech. (2020), *vol*. 900, R4, doi:10.1017/jfm.2020.558

JFM RAPIDS
journals.cambridge.org/rapids

Separation scaling for viscous vortex reconnection

Jie Yao[1] **and Fazle Hussain**[1,†]

[1]Department of Mechanical Engineering, Texas Tech University, Lubbock, TX 79409, USA

(Received 13 April 2020; revised 9 June 2020; accepted 4 July 2020)

Reconnection plays a significant role in the dynamics of plasmas, polymers and macromolecules, as well as in numerous laminar and turbulent flow phenomena in both classical and quantum fluids. Extensive studies in quantum vortex reconnection show that the minimum separation distance δ between interacting vortices follows a $\delta(t) \sim t^{1/2}$ scaling. Due to the complex nature of the dynamics (e.g. the formation of bridges and threads as well as successive reconnections and avalanche), such scaling has never been reported for (classical) viscous vortex reconnection. Using direct numerical simulation of the Navier–Stokes equations, we study viscous reconnection of slender vortices, whose core size is much smaller than the radius of the vortex curvature. For separations that are large compared to the vortex core size, we discover that $\delta(t)$ between the two interacting viscous vortices surprisingly also follows the 1/2-power scaling for both pre- and post-reconnection events. The prefactors in this 1/2-power law are found to depend not only on the initial configuration but also on the vortex Reynolds number (or viscosity). Our finding in viscous reconnection, complementing numerous works on quantum vortex reconnection, suggests that there is indeed a universal route for reconnection – an essential result for understanding the various facets of the vortex reconnection phenomena and their potential modelling, as well as possibly explaining turbulence cascade physics.

Key words: vortex dynamics, vortex interactions, Navier–Stokes equations

1. Introduction

Reconnection, a fundamental topology-transforming event, has been a subject of intense recent study in both classical (Pumir & Kerr 1987; Melander & Hussain 1989; Kida & Takaoka 1994; Kleckner & Irvine 2013) and quantum (Koplik & Levine 1993; Barenghi, Donnelly & Vinen 2001; Bewley *et al.* 2008; Paoletti, Fisher & Lathrop 2010) fluids, as well as in many other fields, such as plasmas (Priest & Forbes 2000), polymers and macromolecules (Vazquez & De Witt 2004). In turbulent flows, vortex reconnection

† Email address for correspondence: fazle.hussain@ttu.edu

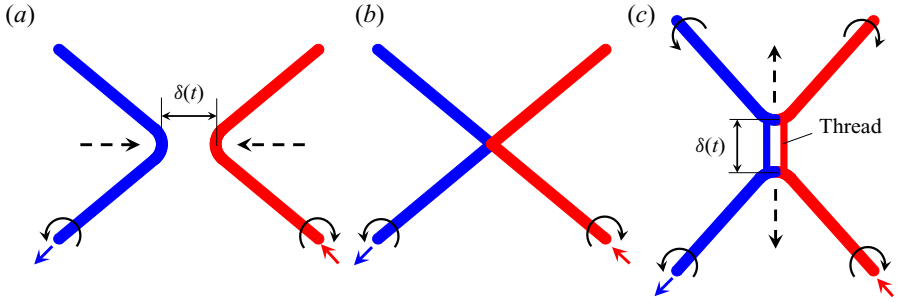

FIGURE 1. Schematic of the evolution of (classical) viscous vortex reconnection: (*a*) before, (*b*) during and (*c*) after reconnection. The curved arrows indicate the rotating directions of the vortices, and the dashed straight arrows represent the directions of vortex motion. Note that the actual reconnection, which is intrinsically three-dimensional, is never complete in classical fluids, leaving unreconnected parts as threads.

appears to be the main mechanism for energy cascade: (i) in quantum fluids, reconnection excites a cascade of Kelvin waves leading to energy dissipation via emissions of phonons and rotons (Kivotides *et al.* 2001; Vinen, Tsubota & Mitani 2003); (ii) in classical fluids, finer and finer scales and turbulence avalanche can occur through successive reconnections (Melander & Hussain 1989; Yao & Hussain 2020*b*). Reconnection is also believed to play an essential role in several other physical phenomena, such as fine-scale mixing (Hussain 1986) and noise generation (Leadbeater *et al.* 2001; Daryan, Hussain & Hickey 2020).

One simple but important question in reconnection is the time scaling of the minimum distance $\delta(t)$ between the two interacting vortices. Assuming that the reconnection is a local process in space and the circulation Γ is the only relevant dimensional quantity involved, dimensional analysis yields

$$\delta(t) = A^{\pm}(\Gamma|t - t_0|)^{1/2}, \tag{1.1}$$

where t_0 is the reconnection time, and A^- and A^+ are dimensionless factors for pre- and post-reconnection, respectively. Such a 1/2-power scaling has been numerically observed for reconnection of line vortices using the Biot–Savart (B–S) law (de Waele & Aarts 1994; Kimura & Moffatt 2017) and also for reconnection of quantized vortices by integrating the Gross–Pitaevksii equation (Nazarenko & West 2003; Villois, Proment & Krstulovic 2017). In addition, recent quantum experiments (Paoletti *et al.* 2010; Fonda, Sreenivasan & Lathrop 2019) confirmed this scaling when the distances between two interacting vortices are large compared with the vortex diameter but small compared with those from other adjacent vortices. Note that deviations from this 1/2 scaling were also reported in several works (Zuccher *et al.* 2012; Allen *et al.* 2014; Rorai *et al.* 2016).

In contrast to the vast literature on the time scaling of $\delta(t)$ in quantum fluids, very limited results have been reported for reconnection in classical fluids, which are governed by the Navier–Stokes (N–S) equations (figure 1). By performing the direct numerical simulation (DNS) of two antiparallel vortex tubes reconnection, Hussain & Duraisamy (2011) found that the minimum distance δ between the vortex centroids scales asymmetrically as $(t_0 - t)^{3/4}$ and $(t - t_0)^2$ before and after the reconnection. Note that in this study, the vortex core size σ is comparable to the initial separation distance δ between these vortices (i.e. $\sigma/\delta \approx 0.4$) – which definitely breaks the local assumption required for the $1/2$ scaling. Inspired by the recent works of Moffatt & Kimura (2019*a*,*b*) on the finite time singularity of Euler and N–S equations, we studied reconnection of two colliding slender vortex rings (the ratio between the initial vortex core size σ and the radius of the ring R is approximately

0.01) and found that $\delta(t)$ before reconnection follows a 1/2 scaling when $\sigma \ll \delta \ll R$ (Yao & Hussain 2020*a*). The main objective of the present work is to further elucidate the time scaling of minimum separation distance for (classical) viscous vortex reconnection. In particular, we want to address the following questions: (i) Does the time scaling of the minimum distance follow $\delta \sim t^{1/2}$ scaling both before and after reconnection? (ii) What dictates the prefactors in the scaling? (iii) What are the similarities/differences between classical and quantum vortex reconnections?

2. Results

Previous studies of the dynamics of slender vortices are mainly based on the vortex filament (VF) method, which is based on the B–S law (Siggia 1985; de Waele & Aarts 1994; Kimura & Moffatt 2018). To regularize the singular kernel of the B–S integral, a cutoff needs to be employed. With such regularization, the B–S integration always diverges near the singular time of reconnection (Villois *et al.* 2017; Kimura & Moffatt 2018). An ad hoc 'cut-and-paste' algorithm is typically required for studying post-reconnection scenarios (Schwarz 1985; Baggaley 2012; Galantucci *et al.* 2019). However, as reconnection in classical fluids is very complex, such an algorithm is very difficult to implement. Hence, the VF method is mainly employed for studying the pre-reconnection event.

With the rapid development of supercomputers these days, DNS for considerably large-scale flow problems are becoming feasible. Here, we aim to employ DNS of the N–S equations for studying viscous reconnection of slender vortices. The numerical method employed here is the same as those used in Yao & Hussain (2020*b*). To understand what is universal in reconnections, three different vortex configurations are considered. Case I is two colliding vortex rings, which is the same as that in Moffatt & Kimura (2019*a*,*b*) and Yao & Hussain (2020*a*) for studying the possible formation of finite time singularity of Euler and N–S equations. Case II is two initially rectilinear, orthogonal vortices, which corresponds to the limit where the radii of curvature κ of two vortices are extremely large. Finally, to study the interaction of vortices with significantly different curvatures, following Galantucci *et al.* (2019), we also consider a case of a vortex ring interacting with an isolated vortex tube (Case III). For all cases, the initial vorticity distribution in the cross-section is assumed to be Gaussian along radial r direction $\omega(r) = \Gamma_0/(4\pi\sigma_0^2)\exp[-r^2/4\sigma_0^2]$ with the circulation $\Gamma_0 = 1$ and core scale $\sigma_0 = 0.01$. Compared with those in the past studies (Melander & Hussain 1989; Boratav, Pelz & Zabusky 1992; Kida & Takaoka 1994; Chatelain, Kivotides & Leonard 2003), the distinction of our simulations is the larger ratio of the radius of curvature to the core size (i.e. $R_0/\sigma_0 \geq 100$). As the viscous effect is an essential issue in classical fluids, for each configuration, two different Reynolds numbers ($Re_\Gamma \equiv \Gamma_0/\nu = 2000$ and 4000), achieved by changing the kinematic viscosity ν, are considered. More technical details are described in the supplementary material and movies available at https://doi.org/10.1017/jfm.2020.558.

2.1. *Colliding vortex rings*

We first consider the interaction of two circular vortex rings, which are symmetrically placed with the initial inclination angle $\theta = \pi/4$ (figure 2*a*). The initial radius of the ring is selected as $R_0 = 1$. In addition, the initial minimum distance between these two vortex rings is chosen as $\delta_0 = 0.2$ so that the interaction between the vortices can be considered as localized ($\sigma_0 \ll \delta_0 \ll R_0$). Note that this vortex set-up represents the typical antiparallel

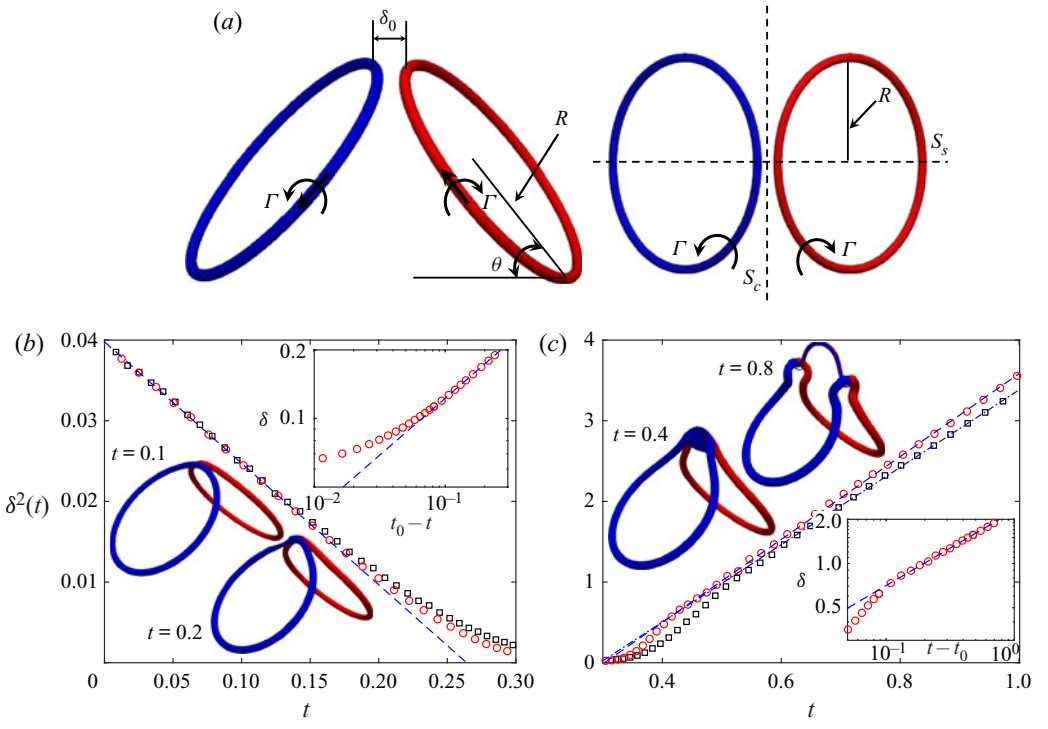

FIGURE 2. Reconnection of colliding vortex rings: (*a*) initial configuration, and evolution of $\delta^2(t)$ at $Re_\Gamma = 2000$ (□) and 4000 (○, red) for (*b*) pre- and (*c*) post-reconnection phases. The blue dashed lines indicate the linear scaling. The insets are flow structures represented by vorticity isosurface at 5 % of maximum initial vorticity $|\boldsymbol{\omega}| = 0.05\omega_0$ for $Re_\Gamma = 2000$; and δ as a function of $|t - t_0|$ for $Re_\Gamma = 4000$ with the dashed line referring the $t^{1/2}$ scaling.

configuration. The evolution of the flow structure for $Re_\Gamma = 2000$ is shown in the insets of figure 2 and also in supplementary movies 1 and 2. The structures for $Re_\Gamma = 4000$, which are quite similar, are not shown due to high computational cost for rendering. Several features that distinctly differ from quantum reconnection deserve to be noted. First, as the rings approach each other under self-induction, they also undergo significant core deformation and form two thin vortex sheets. Second, the reconnection process is not discrete as for quantized vortices, and circulation transfer rate and the reconnection time strongly depend on viscosity ν, and hence on Re_Γ (Hussain & Duraisamy 2011; Yao & Hussain 2020*b*). Finally, reconnection is never complete; as a consequence, the circulation in the reconnected bridges is relatively smaller than the initial circulation Γ_0 of the vortices.

The appropriate determination of $\delta(t)$ relies heavily on the accurate tracking of the location of the vortex axis (Fonda *et al.* 2014; Villois *et al.* 2016), which is rather challenging in classical fluids. First, unlike vortex filaments or quantized vortices, where the axis location is almost precise, the vorticity field in classical fluids is continuously distributed. Second, vortex cores are typically distributed in irregular shapes without any clear centre: before reconnection, the vortices undergo significant core deformation, and, after reconnection, the reconnected vortex lines take some time to collect together to form the bridge.

Due to the twofold symmetry of the initial condition considered, the minimum distance δ between these two interacting rings before and after reconnection should occur in the

Cases	Re_Γ	a^-	t_0^-	a^+	t_0^+
1. Colliding vortex rings	2000	0.38	0.26	2.19	0.30
	4000	0.38	0.26	2.27	0.30
2. Orthogonal vortex tubes	2000	0.29	0.60	0.94	0.65
	4000	0.29	0.61	0.99	0.63
3. Vortex ring and tube	2000	0.39	0.96	1.28	1.09
	4000	0.40	0.93	1.34	1.03

TABLE 1. Fitted values of the prefactors $a^\pm$ and $t_0^\pm$ for the minimum distance scaling $\delta(t) \sim a^\pm |t - t_0^\pm|^{1/2}$. The superscript $\pm$ stands for before $(-)$ and after $(+)$ the reconnection, respectively.

symmetry S_s and collision S_c planes, respectively – which makes the determination of $\delta(t)$ relatively easy. Following Hussain & Duraisamy (2011) and Yao & Hussain (2020*a*), we take the vorticity centroid (computed as the centroid of above 75 % of its maximum) to be the centre for vortices in these two planes. Figure 2(*b*) displays the evolution of $\delta^2(t)$ for the pre-reconnection event, with the top inset showing δ as a function of $t_0 - t$ on a log–log scale for $Re_\Gamma = 4000$. The clear following of linear scaling for $\delta^2(t)$ at the early time suggests that $\delta(t) \sim a^-(t_0^- - t)^{1/2}$, with a^- the constant prefactors for pre-reconnection corresponding to $A^-\Gamma^{1/2}$ in (1.1), and t_0^- the critical time when $\delta \to 0$. For both Re_Γ cases, $\delta^2(t)$ collapses initially and then slowly deviates from linear scaling when $\delta \sim O(\sigma)$. The deviation happens earlier for the $Re_\Gamma = 2000$ case, which is due to the more rapid increase of the core size caused by stronger viscous diffusion. A linear fit on $\delta^2(t)$ between $0 < t < 0.15$ for $Re_\Gamma = 4000$ gives $t_0^- = 0.26$ and $a^- = 0.38$ (table 1). As the circulation remains constant at $\Gamma = 1$ during this time, the dimensionless prefactor $A^- = a^- = 0.38$, which is quite close to $A = 0.4$ reported in de Waele & Aarts (1994).

When two bridges move sufficiently apart from the interacting region, a clear linear scaling for $\delta^2(t)$ can be observed for both Re_Γ cases (figure 2*c*). Hence, $\delta \sim a^+(t - t_0^+)^{1/2}$ scaling also holds in the post-reconnection dynamics when the two bridges' vortices are mainly governed by the mutual interaction. The early evolution of $\delta^2(t)$ deviates from the linear scaling, presumably for two main reasons. First, when the bridges are too close, they are under the influence of other unreconnected structures, such as threads, and other parameters besides Γ may be relevant in determining δ. Second, the reconnected vortex lines, initially in a thin vortex sheet shape, take time to accumulate to form a circular shape, and the circulation Γ continuously increases during this phase. A fit in the linear region gives $t_0^+ \approx 0.30$ for both Re_Γ cases, and $a^+ = 2.19$ and 2.27 for $Re_\Gamma = 2000$ and 4000, respectively (table 1). Different from quantized vortices, where reconnection is discrete and t_0 is almost the same for pre- and post-reconnection, here reconnection is a continuous process, and hence t_0^+ is slightly larger than t_0^-. Consistent with previous studies, a^+ is always larger than a^-, indicating that the vortices separate much faster than their approach. Compared to the pre-reconnection process, the effect of Re_Γ on $\delta(t)$ is more apparent for the post-reconnection. It is because, in classical fluids, the dynamics of reconnection, such as the reconnection time and the circulation transfer rate, strongly depends on the viscosity ν. In general, reconnection is faster at higher Re_Γ, which explains why $\delta^2(t)$ follows linear scaling earlier at $Re_\Gamma = 4000$. In addition, as Re_Γ increases, reconnection is more complete (Yao & Hussain 2020*a*). The variation of a^+ with respect to Re_Γ is

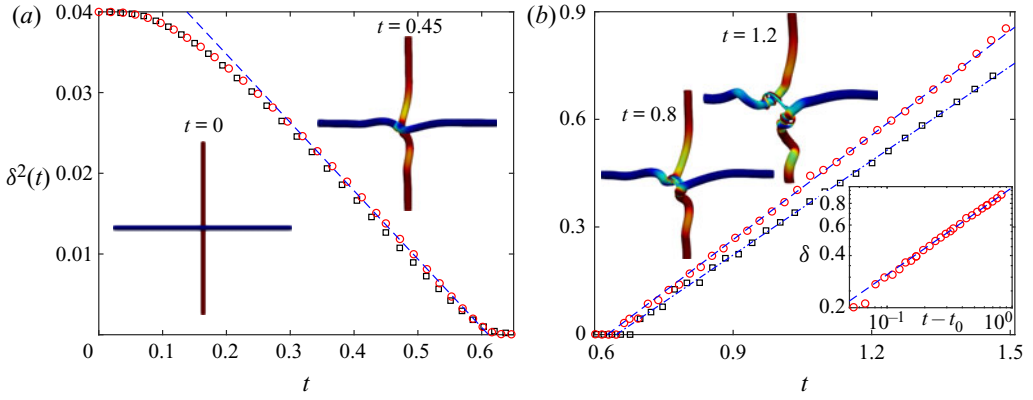

FIGURE 3. Reconnection of orthogonal vortex tubes: time evolution of $\delta^2(t)$ at $Re_\Gamma = 2000$ (□) and 4000 (○, red) for (*a*) the pre- and (*b*) post-reconnection phases, with the dashed lines indicating linear scaling. The insets are flow structures represented by vorticity isosurface $|\boldsymbol{\omega}| = 0.05\omega_0$; the bottom inset in (*b*) is δ as a function of $|t - t_0|$ for $Re_\Gamma = 4000$ with the dashed line indicating the $t^{1/2}$ scaling.

mainly attributed to different circulations Γ in the reconnected bridges – which is difficult to be precisely determined.

2.2. *Orthogonal vortex tubes*

As one of the simplest configurations, the reconnection of orthogonal vortex tubes has been extensively studied for both classical (Boratav *et al.* 1992; Beardsell, Dufresne & Dumas 2016; Jaque & Fuentes 2017) and quantum (Zuccher *et al.* 2012; Galantucci *et al.* 2019) fluids. Similar to Case I, here the initial distance between these two rectilinear vortices is chosen as $\delta_0 = 0.2$. The insets in figures 3(*a*) and 3(*b*) and also supplementary movie 3 show the evolution of the flow structures for $Re_\Gamma = 2000$. The evolution is quite similar to that in Boratav *et al.* (1992) for the thick vortex core case: the vortex tubes first develop into locally antiparallel configuration under mutual induction, then collide with each other due to self-induction; after reconnection, they recede away. Different from quantum cases (Villois *et al.* 2017; Galantucci *et al.* 2019), the unreconnected threads, which wrap around the bridges, are distinct after reconnection. In addition, a Kelvin wave is observed after reconnection. In quantum fluids, nonlinear interaction of Kelvin waves creates waves of shorter and shorter wavelength, which is considered as the main mechanism for energy cascade (Baggaley & Barenghi 2011); in classical fluids, however, the Kelvin wave would rapidly decay due to viscous effect. It would be interesting to compare the difference in the Kelvin wave evolution as well as its role on energy cascade between the quantum and classical reconnections.

To determine the minimum distance $\delta(t)$ between these two vortex tubes, the axis of the vortex tubes needs to be tracked. Here, we propose a vortex tracking method based on the vortex lines that go through the vortex centre at the boundary. First, the centriod of the vortex tubes at the planes $x = -\pi$ and $y = -\pi$ is determined using the same procedure as discussed above. Then, vortex lines that seed from these two centres are integrated using the 'stream3' function in Matlab. Figure 4 (and supplementary movie 4) show the time evolution of the vortex axis for $Re_\Gamma = 2000$, and the evolution at $Re_\Gamma = 4000$ is quantitatively the same. It is clear that the axis of vortex tubes is unambiguously identified. Finally, δ is taken as the shortest distance between these two vortex lines.

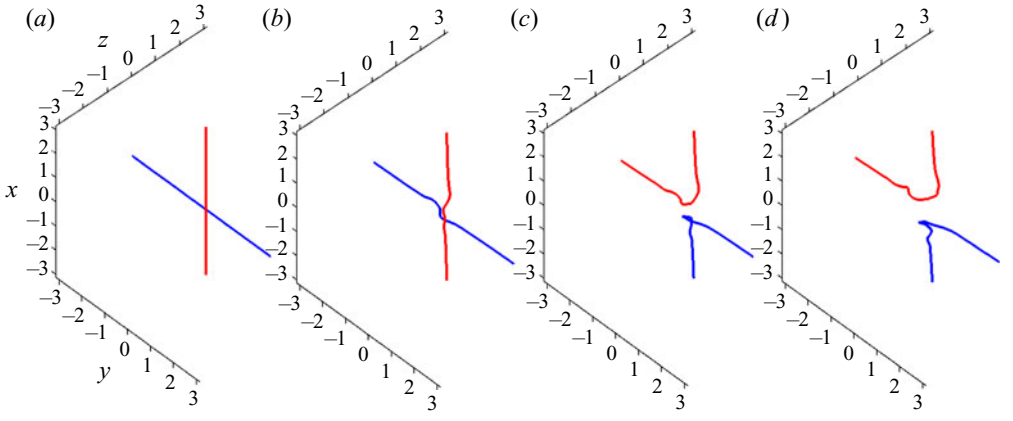

FIGURE 4. Evolution of the vortex axes for the orthogonal vortex tubes case at $Re_\Gamma = 2000$: (*a*) $t = 0$, (*b*) $t = 0.45$, (*c*) $t = 0.8$ and (*d*) $t = 1.2$.

For the pre-reconnection, $\delta^2(t)$ initially varies slowly during the phase of the formation of antiparallel configuration (figure 3*a*). Then, the perturbed vortex tubes approach each other rapidly with $\delta^2(t)$ following a clear linear scaling. A slight difference in the evolution of $\delta^2(t)$ can be observed between $Re_\Gamma = 2000$ and 4000 cases, indicating a weak Reynolds number effect on the pre-reconnection evolution. For both Re_Γ cases, the linear fit shows that $a^- \approx 0.29$, which is slightly smaller than the case of the colliding rings. Figure 3(*b*) shows that $\delta^2(t)$ also follows linear scaling after reconnection, and the $\delta \sim t^{1/2}$ scaling extends far beyond the initial separation distance δ_0. Consistent with Case I, the prefactor increases with Re_Γ, with $a^+ = 0.93$ and 0.99 for $Re_\Gamma = 2000$ and 4000, respectively. Again, the vortices move faster after the reconnection than before it. Similar to the finding in Villois *et al.* (2017), the prefactors a^+ are smaller than those in Case I, which might be due to a smaller curvature of the cusps generated after reconnection in this case.

2.3. *Vortex ring and tube interaction*

The third case we considered is a vortex ring interacting with an isolated rectilinear vortex tube. The radius of the ring is the same as the colliding vortex rings case, namely, $R_0 = 1$. To reveal the cross-over from driven ($\delta \sim t$) to interaction ($\delta \sim t^{1/2}$) region observed in Galantucci *et al.* (2019), the initial distance is chosen as twice the previous cases, namely, $\delta_0 = 0.4$. The vortex set-up and the subsequent evolution for $Re_\Gamma = 2000$ represented by vortex surfaces and tracked vortex axis are shown in the top insets in figures 5(*a*) and 5(*b*), respectively (see also supplementary movies 5 and 6). Due to the self-induction, the vortex ring approaches the vortex tube; during this phase, both the vortex ring and tube are perturbed; at close approach, the vortex ring and tube are also deformed into locally antiparallel configuration (i.e. $t = 1$). It further confirms the argument that reconnection physics of two vortices should be independent of the initial spatial configuration (Siggia & Pumir 1985). After reconnection, parts of the vortex ring and tube exchange with each other, and, due to the Kelvin wave, the newly formed vortex ring and tube become further perturbed with the threads connecting them.

Figure 6(*a*) displays the evolution of $\delta(t)$, with figures 6(*b*) and 6(*c*) showing $\delta^2(t)$ before and after reconnection, respectively. Initially, $\delta(t)$ scales almost linearly with t and the approaching velocity can be approximately determined by the initial self-induced

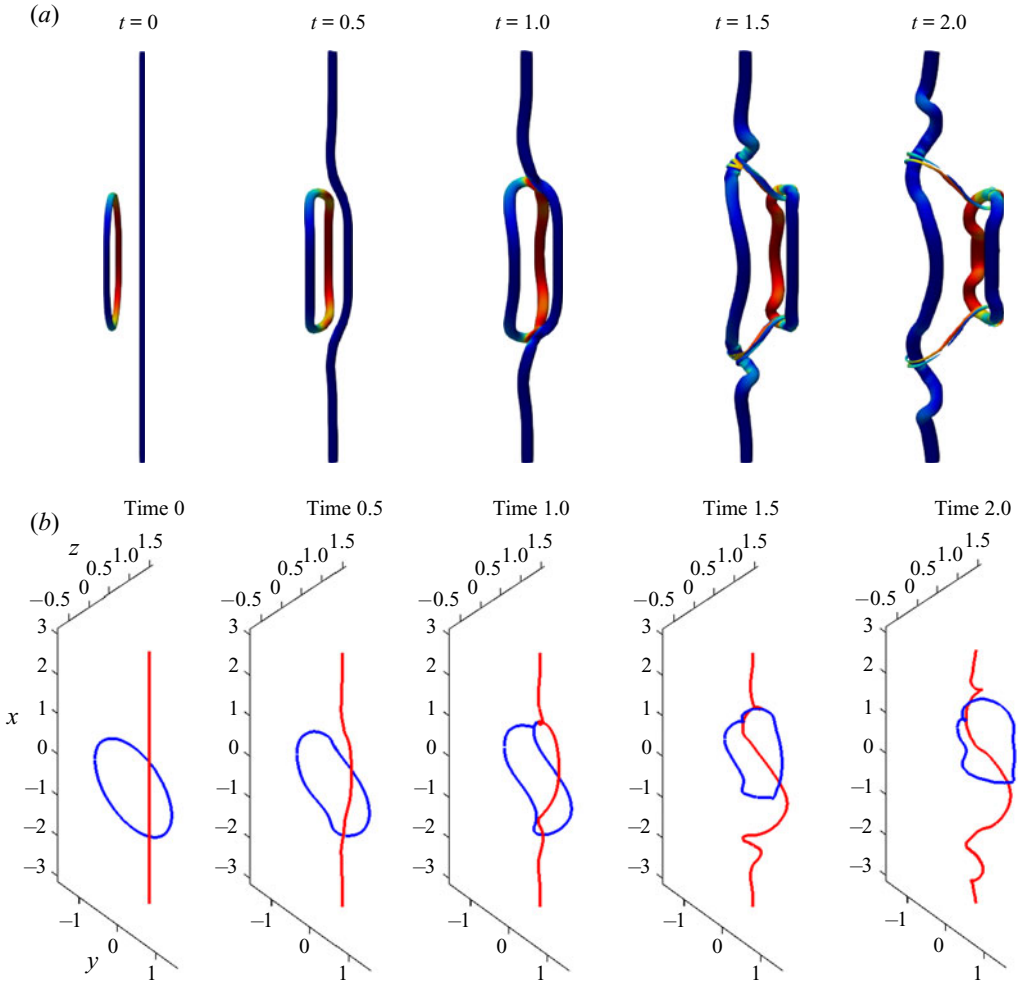

FIGURE 5. Evolution of flow structures for vortex ring and tube interaction for $Re_\Gamma = 2000$: (*a*) represented by vorticity isosurface at 5 % of maximum initial vorticity, i.e. at $|\boldsymbol{\omega}| = 0.05\omega_0$, and (*b*) by tracked vortex axis.

velocity of the ring and the mutual-induced velocity between the ring and the tube. Consistent with the previous two cases, when the two vortices are close to each other, a clear $t^{1/2}$ scaling for δ is observed (inset in figure 6*b*). The transition between driven ($\delta \sim t$) and interaction ($\delta \sim t^{1/2}$) regions happens at $\delta \sim 0.3$. The prefactor for $Re_\Gamma = 4000$ is $a^- = 0.40$, which is very close to Case I.

From figure 6(*c*), it is clear that $\delta(t) \sim t^{1/2}$ scaling holds after reconnection, with the prefactor $a^+ = 1.28$ and 1.34 for $Re_\Gamma = 2000$ and 4000, respectively. The values are between the colliding vortex rings and orthogonal tubes cases. The 1/2 scaling breaks down when the vortex ring moves sufficiently far away from the tube. Note that the cross-over between the $t^{1/2}$ to t^1 scalings for $\delta(t)$ in the post-reconnection is not observed. Instead, for this case $\delta(t)$ remains almost constant after some time. The reason is that the travelling velocity of the perturbed vortex ring is roughly the same as that of the perturbed part of the tube. When the oscillations in the vortex tube and ring die out and the vortex

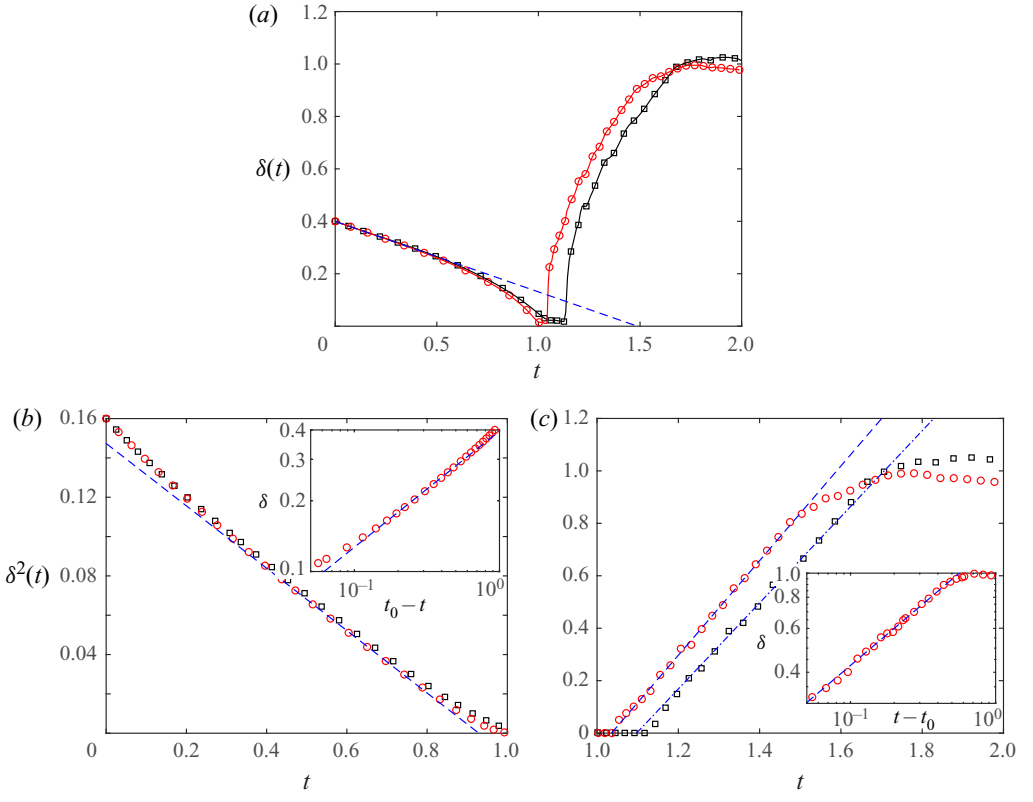

FIGURE 6. Interaction of vortex ring and tube: (*a*) time evolution of $\delta(t)$; and $\delta^2(t)$ for (*b*) the pre-reconnection and (*c*) post-reconnection phases. Symbols □ and ○, red, refer to $Re_\Gamma = 2000$ and 4000, respectively, and the blue dashed lines indicate linear scaling. The insets in (*b*) and (*c*) show separation distance δ as a function of $|t - t_0|$ for $Re_\Gamma = 4000$ with the dashed line indicating the $t^{1/2}$ scaling.

ring regains its circular shape, we should expect $\delta(t) \sim t$ as suggested in Galantucci *et al.* (2019).

3. Conclusions

The question of whether there is a universal scaling/route for reconnection has been extensively studied and debated (Zuccher *et al.* 2012; Villois *et al.* 2017; Fonda *et al.* 2019). Prior works on quantum vortex reconnection have shown clear evidence for the existence of a universal $\delta \sim t^{1/2}$ scaling; however, due to the complex nature for reconnection in classical fluids (presumably due to viscosity), this scaling has never been confirmed previously. With the aid of recent advances in supercomputing, we performed DNS of viscous reconnection for slender vortices at $Re_\Gamma = 2000$ and 4000. Three different initial conditions are considered, namely, two colliding vortex rings; orthogonal and straight vortex tubes; and vortex ring interacting with a tube. For all these cases, the vortices evolve into locally antiparallel configuration – akin to the finding in Villois *et al.* (2017) for the reconnection of quantum vortices. When the distance between two interacting vortices is large compared with their core size, and the dynamics is predominately governed by

their mutual induction, we observe, for the first time, that the approach and separation distances follow a symmetrical 1/2-power scaling, independent of the initial configuration. The discrepancies in previous studies (Hussain & Duraisamy 2011; Yao & Hussain 2020*b*) are due to the fact that the length scale of vortex core size σ is approximately the same order as the separation δ and should be incorporated when considering the scaling. Although the dynamics of the reconnection is substantially different from that in quantum fluids, the surprisingly similar results in classical fluids regarding $\delta(t)$ scaling suggest that there is indeed a universal route towards reconnection. Consistent with previous results (Zuccher *et al.* 2012; Boué *et al.* 2013; Villois *et al.* 2017), we find that the prefactors $a^{\pm}$ in the square root law are not universal and depend on the initial configuration as well as the Reynolds number (or viscosity) – which is a distinct feature for classical vortex reconnection.

Acknowledgements

Computational resources provided by Texas Tech University HPCC, TACC Lonestar and Frontera are acknowledged, and visualization using XSEDE Stampede2 is also appreciated. The original data for the separation distance scaling presented in figures 2–6 can be downloaded from Texas Data Repository Dataverse https://doi.org/10.18738/T8/ONA8DG, and the full flow field data are available from the authors upon reasonable request.

Declaration of interests

The authors report no conflict of interest.

Supplementary material and movies

Supplementary material and movies are available at https://doi.org/10.1017/jfm.2020.558.

References

Allen, A. J., Zuccher, S., Caliari, M., Proukakis, N. P., Parker, N. G. & Barenghi, C. F. 2014 Vortex reconnections in atomic condensates at finite temperature. *Phys. Rev.* A **90** (1), 013601.

Baggaley, A. W. 2012 The sensitivity of the vortex filament method to different reconnection models. *J. Low Temp. Phys.* **168** (1–2), 18–30.

Baggaley, A. W. & Barenghi, C. F. 2011 Spectrum of turbulent Kelvin-waves cascade in superfluid helium. *Phys. Rev.* B **83** (13), 134509.

Barenghi, C. F., Donnelly, R. J. & Vinen, W. F. 2001 *Quantized Vortex Dynamics and Superfluid Turbulence*. Springer Science & Business Media.

Beardsell, G., Dufresne, L. & Dumas, G. 2016 Investigation of the viscous reconnection phenomenon of two vortex tubes through spectral simulations. *Phys. Fluids* **28** (9), 095103.

Bewley, G. P., Paoletti, M. S., Sreenivasan, K. R. & Lathrop, D. P. 2008 Characterization of reconnecting vortices in superfluid helium. *Proc. Natl Acad. Sci.* **105** (37), 13707–13710.

Boratav, O. N., Pelz, R. B. & Zabusky, N. J. 1992 Reconnection in orthogonally interacting vortex tubes: direct numerical simulations and quantifications. *Phys. Fluids* A **4** (3), 581–605.

Boué, L., Khomenko, D., L'vov, V. S. & Procaccia, I. 2013 Analytic solution of the approach of quantum vortices towards reconnection. *Phys. Rev. Lett.* **111** (14), 145302.

CHATELAIN, P., KIVOTIDES, D. & LEONARD, A. 2003 Reconnection of colliding vortex rings. *Phys. Rev. Lett.* **90** (5), 054501.

DARYAN, H., HUSSAIN, F. & HICKEY, J.-P. 2020 Aeroacoustic noise generation due to vortex reconnection. *Phys. Rev. Fluids* **5**, 062702.

FONDA, E., MEICHLE, D. P., OUELLETTE, N. T., HORMOZ, S. & LATHROP, D. P. 2014 Direct observation of Kelvin waves excited by quantized vortex reconnection. *Proc. Natl Acad. Sci.* **111**, 4707–4710.

FONDA, E., SREENIVASAN, K. R. & LATHROP, D. P. 2019 Reconnection scaling in quantum fluids. *Proc. Natl Acad. Sci.* **116** (6), 1924–1928.

GALANTUCCI, L., BAGGALEY, A. W., PARKER, N. G. & BARENGHI, C. F. 2019 Crossover from interaction to driven regimes in quantum vortex reconnections. *Proc. Natl Acad. Sci.* **116** (25), 12204–12211.

HUSSAIN, A. K. M. F. 1986 Coherent structures and turbulence. *J. Fluid Mech.* **173**, 303–356.

HUSSAIN, F. & DURAISAMY, K. 2011 Mechanics of viscous vortex reconnection. *Phys. Fluids* **23** (2), 021701.

JAQUE, R. S. & FUENTES, O. V. 2017 Reconnection of orthogonal cylindrical vortices. *Eur. J. Mech. B/Fluids* **62**, 51–56.

KIDA, S. & TAKAOKA, M. 1994 Vortex reconnection. *Annu. Rev. Fluid Mech.* **26** (1), 169–177.

KIMURA, Y. & MOFFATT, H. K. 2017 Scaling properties towards vortex reconnection under Biot–Savart evolution. *Fluid Dyn. Res.* **50** (1), 011409.

KIMURA, Y. & MOFFATT, H. K. 2018 A tent model of vortex reconnection under Biot–Savart evolution. *J. Fluid Mech.* **834**, R1.

KIVOTIDES, D., VASSILICOS, J. C., SAMUELS, D. C. & BARENGHI, C. F. 2001 Kelvin waves cascade in superfluid turbulence. *Phys. Rev. Lett.* **86** (14), 3080–3083.

KLECKNER, D. & IRVINE, W. T. M. 2013 Creation and dynamics of knotted vortices. *Nat. Phys.* **9** (4), 253–258.

KOPLIK, J. & LEVINE, H. 1993 Vortex reconnection in superfluid helium. *Phys. Rev. Lett.* **71** (9), 1375–1378.

LEADBEATER, M., WINIECKI, T., SAMUELS, D. C., BARENGHI, C. F. & ADAMS, C. S. 2001 Sound emission due to superfluid vortex reconnections. *Phys. Rev. Lett.* **86** (8), 1410–1413.

MELANDER, M. V. & HUSSAIN, F. 1989 Cross-linking of two antiparallel vortex tubes. *Phys. Fluids* A **1** (4), 633–636.

MOFFATT, H. K. & KIMURA, Y. 2019*a* Towards a finite-time singularity of the Navier–Stokes equations. Part 1. Derivation and analysis of dynamical system. *J. Fluid Mech.* **861**, 930–967.

MOFFATT, H. K. & KIMURA, Y. 2019*b* Towards a finite-time singularity of the Navier–Stokes equations. Part 2. Vortex reconnection and singularity evasion. *J. Fluid Mech.* **870**, R1.

NAZARENKO, S. & WEST, R. 2003 Analytical solution for nonlinear Schrödinger vortex reconnection. *J. Low Temp. Phys.* **132** (1–2), 1–10.

PAOLETTI, M. S., FISHER, M. E. & LATHROP, D. P. 2010 Reconnection dynamics for quantized vortices. *Physica* D **239** (14), 1367–1377.

PRIEST, E. & FORBES, T. 2000 *Magnetic Reconnection: MHD Theory and Applications*. Cambridge University Press.

PUMIR, A. & KERR, R. M. 1987 Numerical simulation of interacting vortex tubes. *Phys. Rev. Lett.* **58** (16), 1636–1639.

RORAI, C., SKIPPER, J., KERR, R. M. & SREENIVASAN, K. R. 2016 Approach and separation of quantised vortices with balanced cores. *J. Fluid Mech.* **808**, 641–667.

SCHWARZ, K. W. 1985 Three-dimensional vortex dynamics in superfluid ^{4}He: line–line and line–boundary interactions. *Phys. Rev.* B **31** (9), 5782–5804.

SIGGIA, E. D. 1985 Collapse and amplification of a vortex filament. *Phys. Fluids* **28** (3), 794–805.

SIGGIA, E. D. & PUMIR, A. 1985 Incipient singularities in the Navier–Stokes equations. *Phys. Rev. Lett.* **55** (17), 1749–1752.

VAZQUEZ, M. & DE WITT, S. 2004 Tangle analysis of gin site-specific recombination. *Math. Proc. Camb. Phil. Soc.* **136**, 565–582.

VILLOIS, A., KRSTULOVIC, G., PROMENT, D. & SALMAN, H. 2016 A vortex filament tracking method for the Gross–Pitaevskii model of a superfluid. *J. Phys.* A **49** (41), 415502.

VILLOIS, A., PROMENT, D. & KRSTULOVIC, G. 2017 Universal and nonuniversal aspects of vortex reconnections in superfluids. *Phys. Rev. Fluids* **2** (4), 044701.

VINEN, W. F., TSUBOTA, M. & MITANI, A. 2003 Kelvin-wave cascade on a vortex in superfluid ^{4}He at a very low temperature. *Phys. Rev. Lett.* **91** (13), 135301–135304.

DE WAELE, A. T. A. M. & AARTS, R. G. K. M. 1994 Route to vortex reconnection. *Phys. Rev. Lett.* **72**, 482–485.

YAO, J. & HUSSAIN, F. 2020*a* On singularity formation via viscous vortex reconnection. *J. Fluid Mech.* **888**, R2.

YAO, J. & HUSSAIN, F. 2020*b* A physical model of turbulence cascade via vortex reconnection sequence and avalanche. *J. Fluid Mech.* **883**, A51.

ZUCCHER, S., CALIARI, M., BAGGALEY, A. W. & BARENGHI, C. F. 2012 Quantum vortex reconnections. *Phys. Fluids* **24** (12), 125108.